Available online at www.sciencedirect.com

SCIENCE DIRECT®

Thermochimica Acta 409 (2004) 177–187

thermochimica acta

www.elsevier.com/locate/tca

Zinc ions and zinc sulfide particles in sol–gel zirconium phosphate synthesis, thermal behavior and X-ray characterization

C. Ferragina[a,*], R. Di Rocco[a], L. Petrilli[b]

[a] Istituto di Metodologie Inorganiche e dei Plasmi, Via Salaria Km 29.300, 00016 Monterotondo, Rome, Italy
[b] Istituto Struttura della Materia, C.N.R., Via Salaria Km 29.300, 00016 Monterotondo, Rome, Italy

Received 25 March 2003; received in revised form 4 June 2003; accepted 17 June 2003

Abstract

Zinc ions can be exchanged in sol–gel zirconium phosphate by using the batch or hydrothermal method. The zinc materials obtained that undergo thermal treatment after complete dehydration, can rehydrate fully or partially depending on whether half or all the zinc ions are exchanged. At high temperature syntherization is evident. By flowing sulfide acid over the zinc forms, zinc sulfide particles are formed and their amount depends on the length of time of the gas flow and on the state of hydration of the original material. This is not the case in the half exchanged zinc zirconium phosphate material. The decomposition temperature of the ZnS particles depends on their position in the exchanger: whether on the surface or between the layers of the host matrix. The XRD patterns of the materials obtained are similar to those of the sol–gel zirconium phosphate. The presence of ZnS particles is evident.

Keywords: Ion-exchanger; Intercalation; Layered compound; Thermal behavior; ZnS

---

1. Introduction

There is a growing interest in acid phosphates of tetravalent elements because of their properties both to exchange ions [1] and to intercalate molecules [2], complexes [3], and long chain surfactants [4]. An inorganic ion-exchanger α-zirconium phosphate [α-Zr(HPO_4)$_2$·H_2O: α-ZrP], is known to have a layered structure with interlayer spacing *d* of 7.56 Å [5]. This allows the intercalation processes to take place between the layers. The intercalation compounds derived are of increasing importance in producing nanocomposite multifunctional materials, which can enhance catalytic activity [6], adsorptive capacity [7] or as a support for quantum-well particles [8a]. As in the case of zeolites [9], the dimension of the zirconium phosphate host matrix can be modulated to accept quantum size particles such as CdS or ZnS [8a]. The semiconductors ZnS and CdS are used widely in solar cellar technology as an optical coatings and as a display devices [9]. Furthermore these semiconductors are of photoconductive, luminescent and piezoelectric. IR window and lens, a photoconductor, a solar cell and a light emitting diode material are some of the potential applications of ZnS [9]. This paper describes the synthesis and characterization of α-ZrP, synthesized with the sol–gel (SG) method. The procedure adopted was similar to that used in previous works involving CdS in the same host matrix [8b].

2. Experimental procedure

2.1. Chemicals

Zinc acetate dihydrate, zinc nitrate tetrahydrate and iron sulfide were purchased as pure grade reagents from Aldrich and used without any further purification. All the other reagents used were Merck pro analyze products.

2.2. Materials

Crystalline sol–gel zirconium phosphate (SGZrP) was synthesized as reported in the literature [10]. The zinc sol–

---

[*] Corresponding author. Tel.: +36-06-90672225; fax: +39-06-90672238.
E-mail address: carla.ferragina@mlib.cnr.it (C. Ferragina).

0040-6031/$ – see front matter © 2003 Elsevier B.V. All rights reserved.
doi:10.1016/S0040-6031(03)00360-5

gel zirconium phosphate (SGZrPZn) was prepared by ion-exchange, using both: the batch and hydrothermal methods.

The zinc sulfide zirconium phosphate (SGZrPZnS) materials were obtained by flowing anhydrous H_2S over the partially or fully dehydrate zinc forms, for varying lengths of time and at different dehydration temperatures.

2.3. Physical measurements and chemical analysis

A GBC 903 A.A. spectrophotometer was used to analyze the zinc solutions ions before and after the batch contact with the ion-exchanger. The phosphate content was determined colorimetrically [11].

The water content and thermal behavior of the materials obtained were examined using a simultaneous TG-DTA Stanton Redcroft 1500 thermoanalyzer, Pt crucibles, heat ranging from $10\,^{\circ}\mathrm{C\,min^{-1}}$ up to $1100\,^{\circ}\mathrm{C}$ in an air flow.

In order to study the phase changes that the materials underwent a Philips diffractometer X-ray powder diffraction (model PW 1130/00) with Ni-filtered Cu Kα radiation ($\lambda = 1.541$ Å) was used to monitor the d reflection and its harmonics.

The content of sulfur and hydrogen ions present in the materials, was determined with a Fisions 1108 elemental microanalyzer.

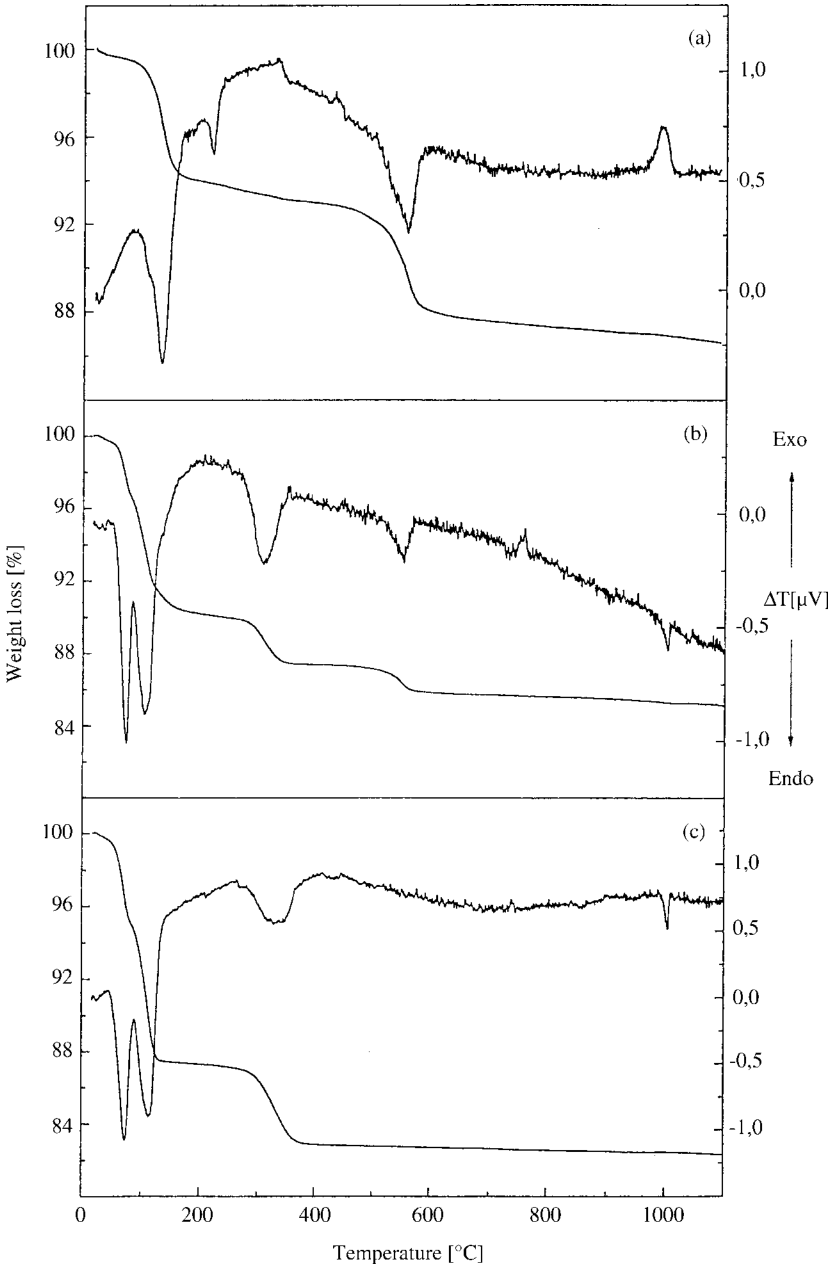

Fig. 1. TG-DTA curves of: (a) SGZrP; (b) SGZrPZn$_{0.50}$; (c) SGZrPZn.

3. Results and discussion

3.1. Zinc materials derived by SGZrP

In previous work [12], the zinc zirconium phosphate material was prepared by the batch method, using a sodium ion-containing phase, at room temperature (r.t.). In this experiment, the material is prepared by contacting samples of 1 mmol of SGZrP with volumes of 22 ml of 4.5×10^{-2} mol dm^{-3} of a zinc acetate solution, or nitrate solution, for a week, at 45 °C. The aim was to obtain a fully exchanged SGZrPZn phase. The solid is separated from the solution by centrifugation and dried by exposing it to r.t. Using a zinc acetate solution the exchange is 100%, whereas using a zinc nitrate solution the exchange is very poor (∼27%).

The typical procedure to obtain the exchanged materials by hydrothermal synthesis is by contacting samples of 1 mmol of SGZrP with volumes of 22 ml of 4.5×10^{-2} mol dm^{-3} of zinc acetate solution. The solid solution is put into a sealed and charged Pyrex tube and placed in a hydrothermal bomb and heated in an oven, for 3 days, thermostatted to ±10 °C, at 120 °C. After cooling, the bomb is opened and the solid is filtered and dried by exposing it to r.t. The exchange between the zinc ions and the hydrogen of the POH groups is 100%. A complete exchange cannot be achieved in fewer than 3 days or at

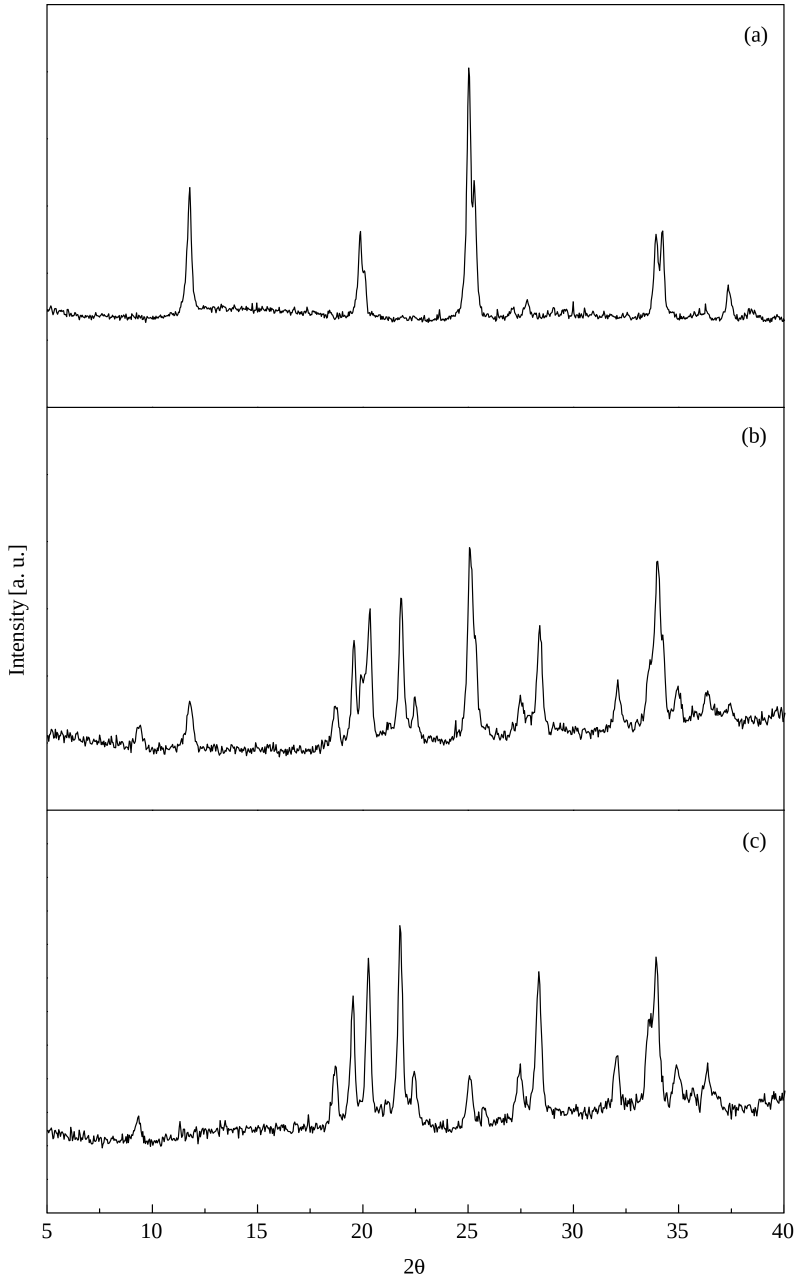

Fig. 2. XRDP of: (a) SGZrP; (b) SGZrPZn$_{0.50}$; (c) SGZrPZn.

a temperature below 80 °C. The chemical formula of the fully exchanged zinc form obtained using the two methods is $SGZr(PO_4)_2Zn{\cdot}4H_2O$ (SGZrPZn).

A half exchanged zinc form is also prepared by contacting sample of 1 mmol of SGZrP with a volume of 11 ml of 4.5×10^{-2} mol dm^{-3} of a zinc acetate solution. The chemical formula of the material obtained is $SGZrZn_{0.50}(H_{0.50}PO_4)_2{\cdot}2H_2O$ ($SGZrPZn_{0.50}$).

3.2. Thermal behavior of the zinc materials

The materials obtained underwent thermal treatment. Fig. 1 shows the simultaneous TG-DTA curves of the $SGZrPZn_{0.50}$ and SGZrPZn materials compared to that of SGZrP. In the case of a fully exchanged material, it is evident from the TG curve that the four water molecules are lost in three distinct stages between 25 and 450 °C. The amount of loss varies: loss of $1.30H_2O$, $1.70H_2O$ and H_2O and occur, respectively, between 25 and 80 °C, 80 and 220 °C, and 220 and 450 °C. The first two losses occur in a relatively short time and consecutively, whereas the last one is more gradual and occurs at a higher temperature. The material fully dehydrated at 450 °C rehydrates up to 77% when exposed to r.t. for 1 day. The DTA curve confirms the TG data showing three endothermic peaks which represent water loss. Between 950 and 1050 °C, on the DTA curve, an endothermic

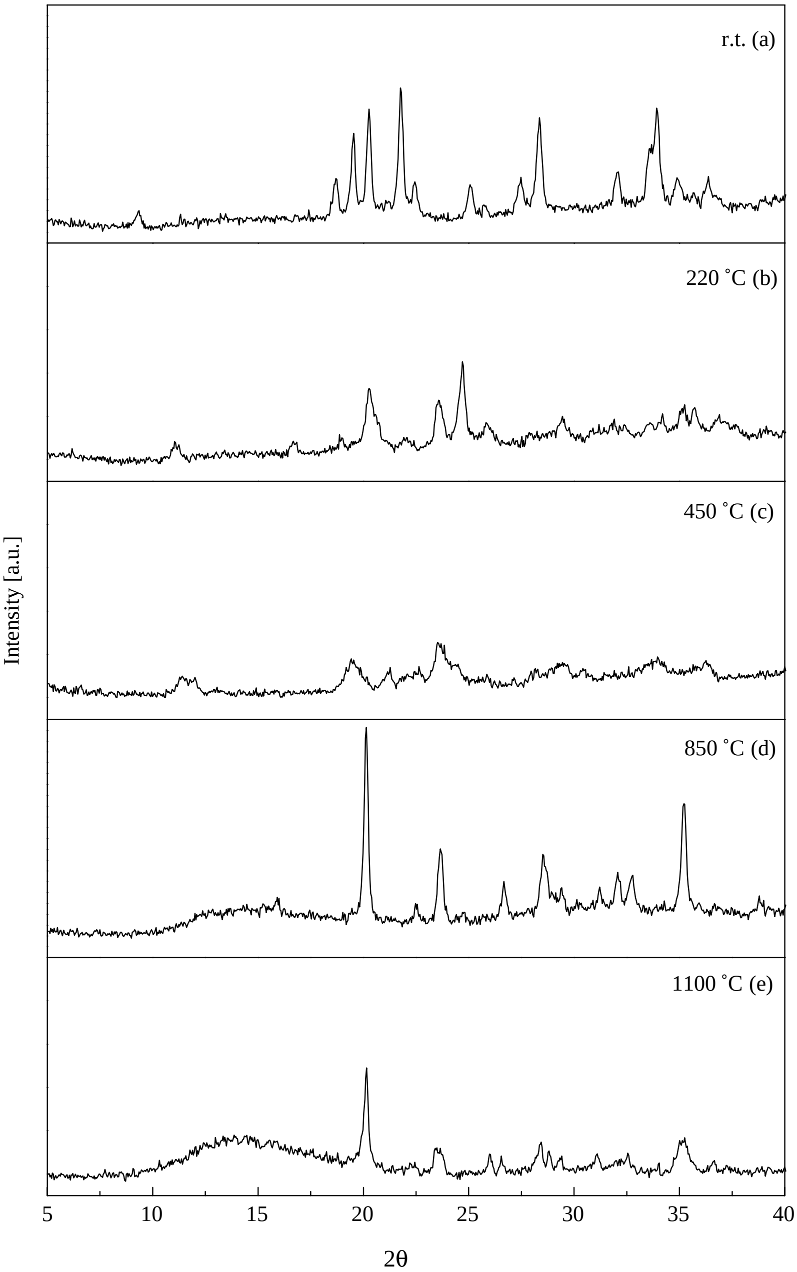

Fig. 3. XRDP of SGZrPZn at various temperature: (a) r.t.; (b) 220 °C; (c) 450 °C; (d) 850 °C; (e) 1100 °C.

sharp peak is evident, without a correspondent weight loss on the TG curve: this is due to a transition phase (syntherization). In fact at 1100 °C the residual material is like glass.

As regards $SGZrPZn_{0.50}$, on the TG curve, between 25 and 450 °C, three weight losses are shown at the same temperature ranges as above, but the amount of loss is different: $0.54H_2O$, H_2O and $0.46H_2O$. This is due to the water co-ordination. Between 450 and 650 °C, there is also a further loss due to the water from the condensation of the POH groups, not involved in the Zn^{2+} ions exchange. The DTA curve is in accordance with the TG data showing four endothermic peaks indicating a loss of water. An exothermic peak at 750 °C, related to the pyrophosphate formation [5c], and an endothermic peak, at 980 °C, related to the syntherization of the zinc phosphate obtained, are evident. The condensation of the POH groups, necessary to give pyrophosphate, in this material occurs at a lower temperature than that of SGZrP (Fig. 1a), whereas the water loss resulting from the condensation of the POH groups occurs at the same temperature. The dehydrate material rehydrates almost 100% (92%) when exposed to r.t. for 1 day.

3.3. XRD pattern of the zinc materials

In Fig. 2, comparison between the XRD patterns of SGZrPZn, $SGZrPZn_{0.5}$ and SGZrP is reported. An increase in *d*

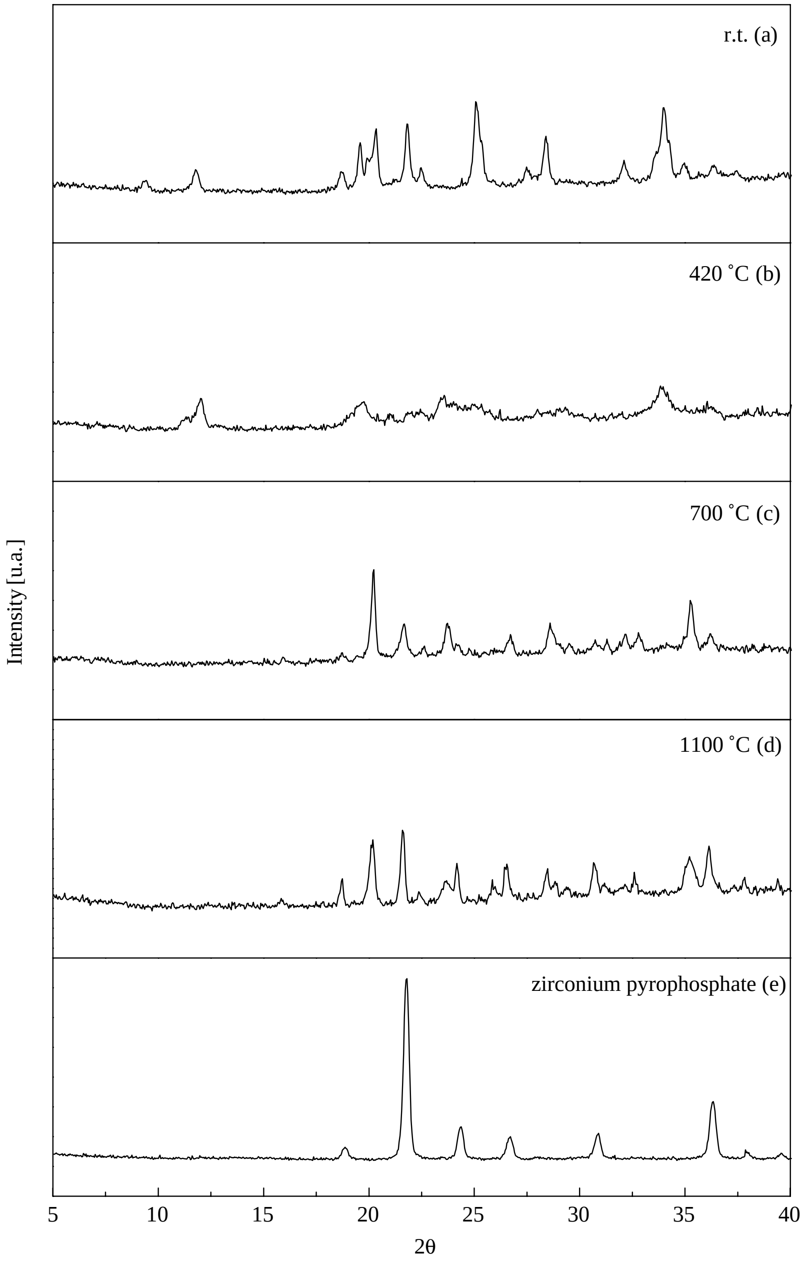

Fig. 4. XRDP of $SGZrPZn_{0.50}$ at various temperature: (a) r.t.; (b) 420 °C; (c) 700 °C; (d) 1100 °C; (e) SGZrP cubic pyrophosphate 1100 °C.

Table 1
mass% S and mass% H of the zinc materials submitted to the H_2S gas over the time[a]

Materials	8 h		15 h		25 h		50 h		Approximate chemical formula
	mass% S	mass% H	mass% S	mass% H	mass% S	mass% H	mass% S	mass% H	
SGZrPZnS$_{220}$	2.99 (0.29ZnS)	0.92 (0.29ZnS)	4.35 (0.43ZnS)	0.92 (0.43ZnS)	4.22 (0.43ZnS)	0.93 (0.43ZnS)	5.38 (0.57ZnS)	0.94 (0.57ZnS)	$Zr(H_{0.57}PO_4)_2Zn_{0.43}$ $(ZnS)_{0.57}\cdot 1.21H_2O$
SGZrPZnS$_{450}$	1.74 (0.16ZnS)	0.85 (0.16ZnS)	2.38 (0.23ZnS)	0.98 (0.23ZnS)	3.0 (0.36ZnS)	1.11 (0.36ZnS)	7.05 (0.79ZnS)	0.76 (0.79ZnS)	$Zr(H_{0.79}PO_4)_2Zn_{0.21}$ $(ZnS)_{0.79}\cdot 1.65H_2O$
SGZrPZn$_{0.50}$ (after H_2S gas flow)	0	1.07	0	1.04	0	0.98	0	0.94	$Zr(H_{0.50}PO_4)_2Zn_{0.50}\cdot$ $1.65H_2O$

[a] The values in brackets represents mol ZnS/mol exchanger SGZrP.

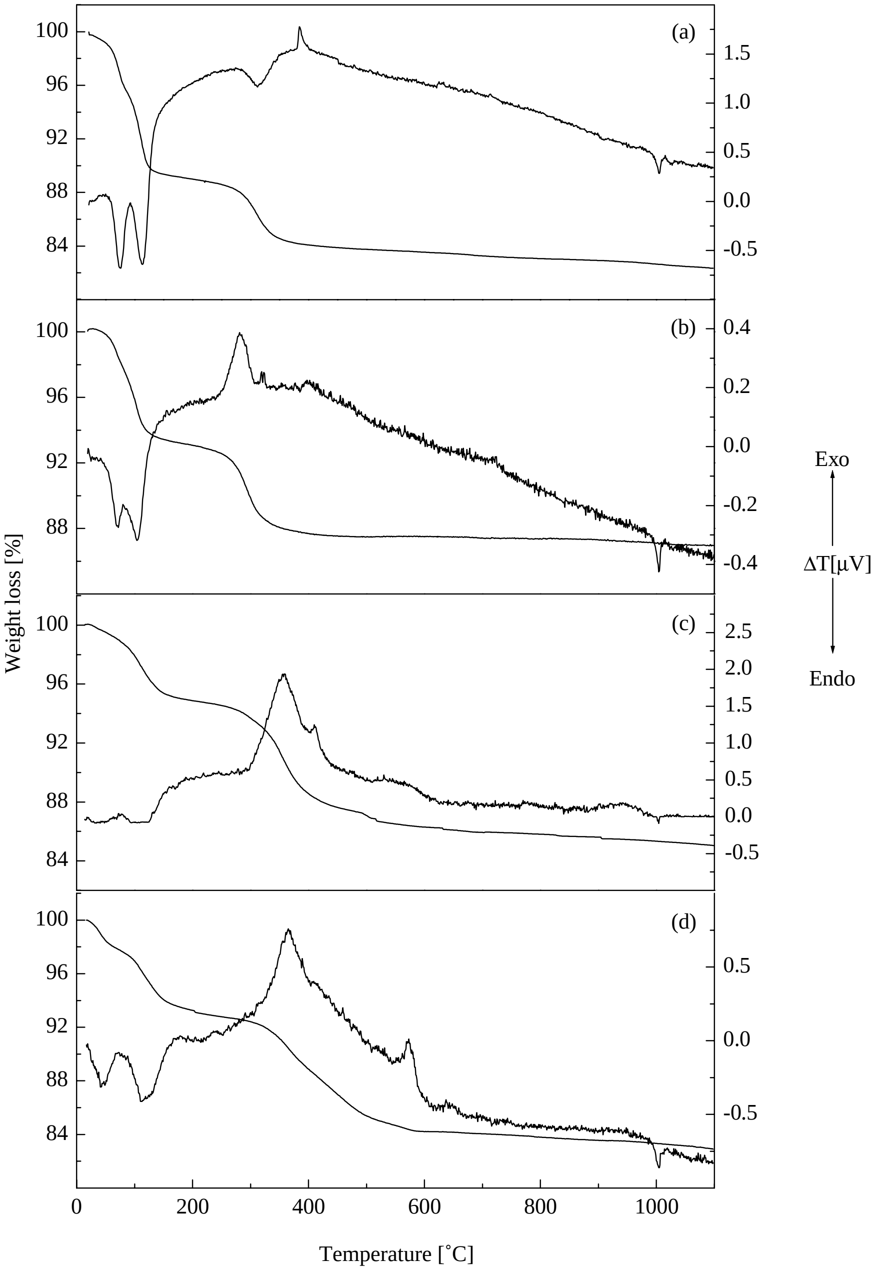

Fig. 5. TG-DTA curves of the SGZrPZnS$_{450}$ at different length of time of flowing H_2S: (a) 8 h; (b) 15 h; (c) 25 h; (d) 50 h.

Table 2
mass% S and mass% H (for SGZrPZnS$_{450}$) present after the first and second surfactant loss[a,b]

Material	380 °C		450 °C		580 °C	
	mass% S	mass% H	mass% S	mass% H	mass% S	mass% H
SGZrPZnS$_{450}$	6.12 (0.66ZnS) [0.13ZnS]	1.04 (0.66ZnS) [0.13ZnS]	2.41 (0.23ZnS) [0.43ZnS]	1.67 (0.23ZnS) [0.43ZnS]	0 (0) [0.23ZnS]	0.94 (0) [0.23ZnS]

[a] The values in round brackets represent ZnS particles present at 380 and 450 °C in the SGZrP.
[b] The values in square brackets represent ZnS particles lost.

in the fully exchanged material with respect to that of its precursor SGZrP (9.56 vs. 7.56 Å) is evident. The resulting diffractogram is similar but less crystalline than that reported in literature [12]. The spectra of SGZrPZn performed at r.t. (Fig. 3a) and at the dehydration temperatures (Fig. 3b and c) before and after synthesization (Fig. 3d and e) show that there is no variation up to the first stage of water loss (this spectrum is equal to that recorded at r.t.), whereas at the second stage of water loss at 220 °C a decrease in *d* (8.07 Å) is noted and a different diffractogram is evident. At 450 °C, when dehydration is complete, the diffractogram becomes more amorphous with a double phase 7.76–7.37 Å (a little different from the value reported in the literature [12]). This rehydrated material shows a spectrum exactly the same as that recorded at r.t. At 700 °C, the formation of zinc zirconium double phosphate [12,13] is evident. At 800 °C,

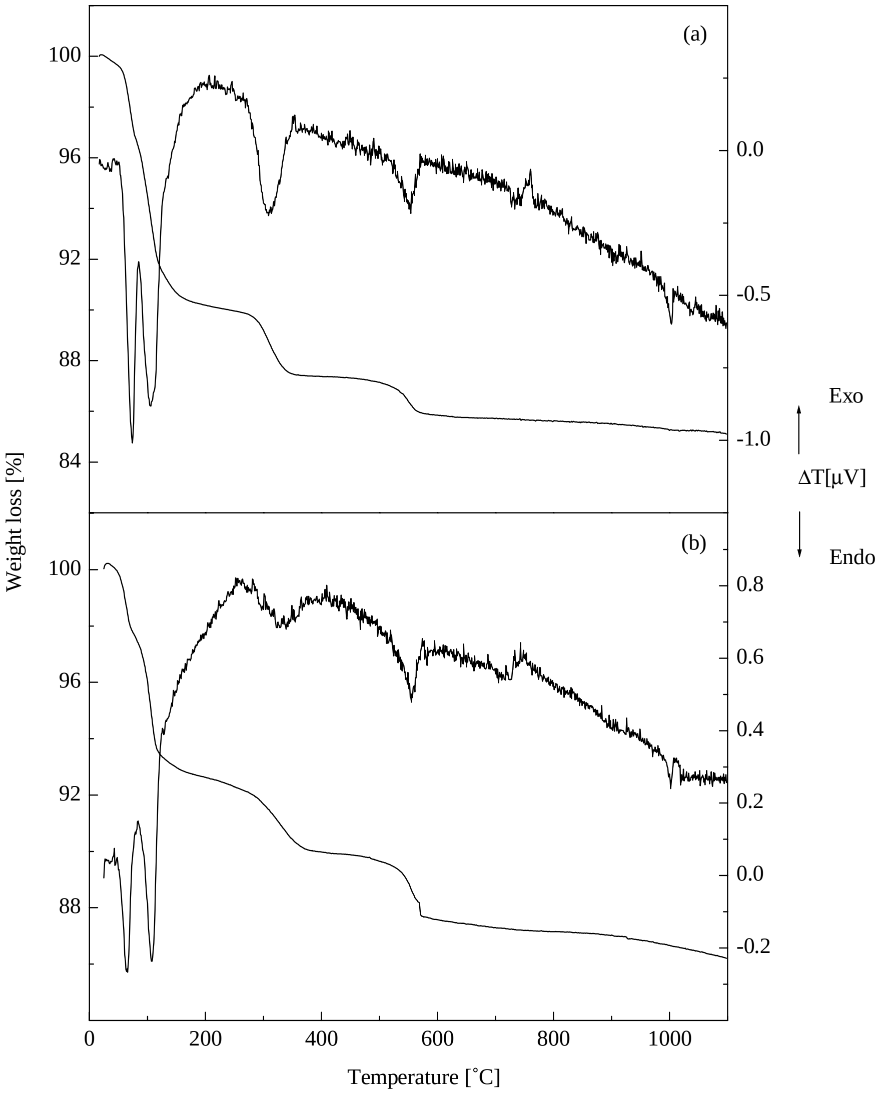

Fig. 6. TG-DTA curves of SGZrPZn$_{0.50}$ (a) and SGZrPZn$_{0.50}$ after gas flow (b) for comparison.

some changes in the pattern occur at 2θ angles between 24° and 45°, indicating the presence of zinc zirconium double phosphate and the beginning of syntherization. At 1100 °C, when the material is fully synthesized, only a few changes are evident.

The XRD pattern of SGZrPZn$_{0.50}$ shows peaks both of SGZrPZn and SGZrP (Fig. 4a). After dehydration at 420 °C (Fig. 4b) a double phase is present with peaks at 7.83 and 7.37 Å. The rehydrated material shows a diffractogram similar to that obtained at r.t. At 700 °C and at 1100 °C, both zinc zirconium double phosphate salt (Fig. 3e) and cubic pyrophosphate (Fig. 4e) are evident [5c].

3.4. Zinc sulfide materials derived by SGZrPZn

The general procedure to produce ZnS particles in SGZrPZn (SGZrPZnS) can be summarized as follows: anhydrous H_2S is made to flow for varying lengths of time (1–50 h) at r.t. over samples of 1 mmol of SGZrPZn calcinated at 220 or 450 °C (SGZrPZnS$_{220}$, SGZrPZnS$_{450}$), respectively, when partially (two water molecules still present) or completely dehydrated. The anhydrous H_2S was obtained by reacting FeS with HCl and by dehydrating the gas over two columns containing H_2SO_4 and $CaSO_4$. The aim was to establish the importance of the presence of water in SGZrPZn in producing ZnS. As has already been noted (see before) after

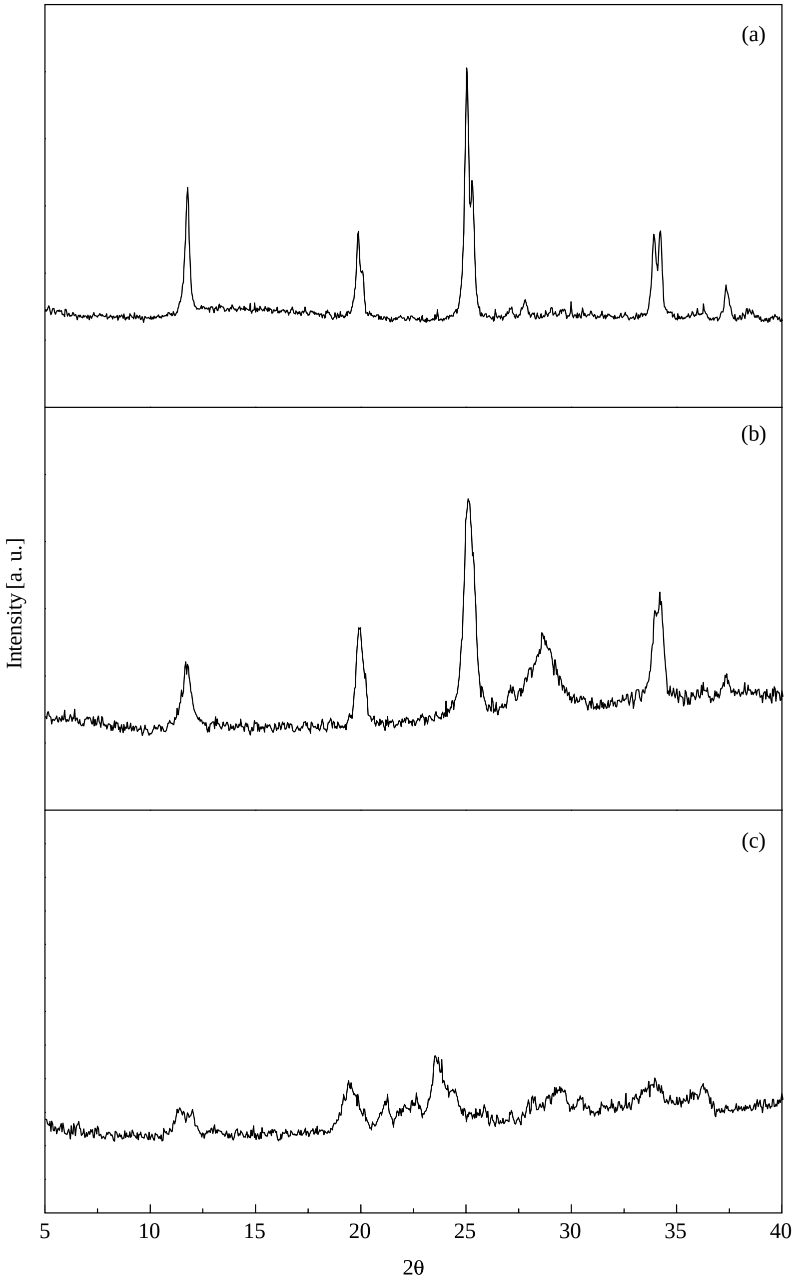

Fig. 7. XRDP of: (a) SGZrP; (b) SGZrPZnS$_{450}$; (c) SGZrPZn heated at 450 °C.

dehydration of SGZrPZn, there is a decrease in *d* (9.56 vs. 8.07 Å, 9.56 vs. 7.76–7.37 Å) in material heated at 220 and 450 °C, respectively. The incoming gas reacts with the zinc ions of the phosphate groups to obtain ZnS particles because of an ion-exchange between the H^+ of the H_2S and Zn^{2+} ions of the phosphate groups. Unlike in the case of the CdS [8b], the color of the material remains white. Table 1 reports the ZnS content in $SGZrPZn_{220}$ and $SGZrPZn_{450}$. It is evident that in both materials not all the Zn^{2+} previously exchanged was utilized to obtain ZnS. The microanalysis data show that the sulfur content increases due to an increase in the length of time of the gas flow and a decrease in the water co-ordination. The thermal behavior and the XRD patterns of the resulting materials also depend on the length of time of the gas flow (Figs. 5 and 7, respectively).

An experiment with H_2S was also performed on the $SGZrPZn_{0.50}$ material, calcinated at 450 °C. The aim was to find out what would be the difference in results in producing ZnS in a half exchanged material (with less steric hindrance of zinc ions). As reported in Table 1, no ZnS formation is evident in this case. In fact it is difficult, for H_2S gas flow, to exchange Zn^{2+} ions to produce ZnS in a matrix where there is a fair number of H^+ ions (not exchanged with the Zn^{2+} ions). The ion-exchange H^+ (from

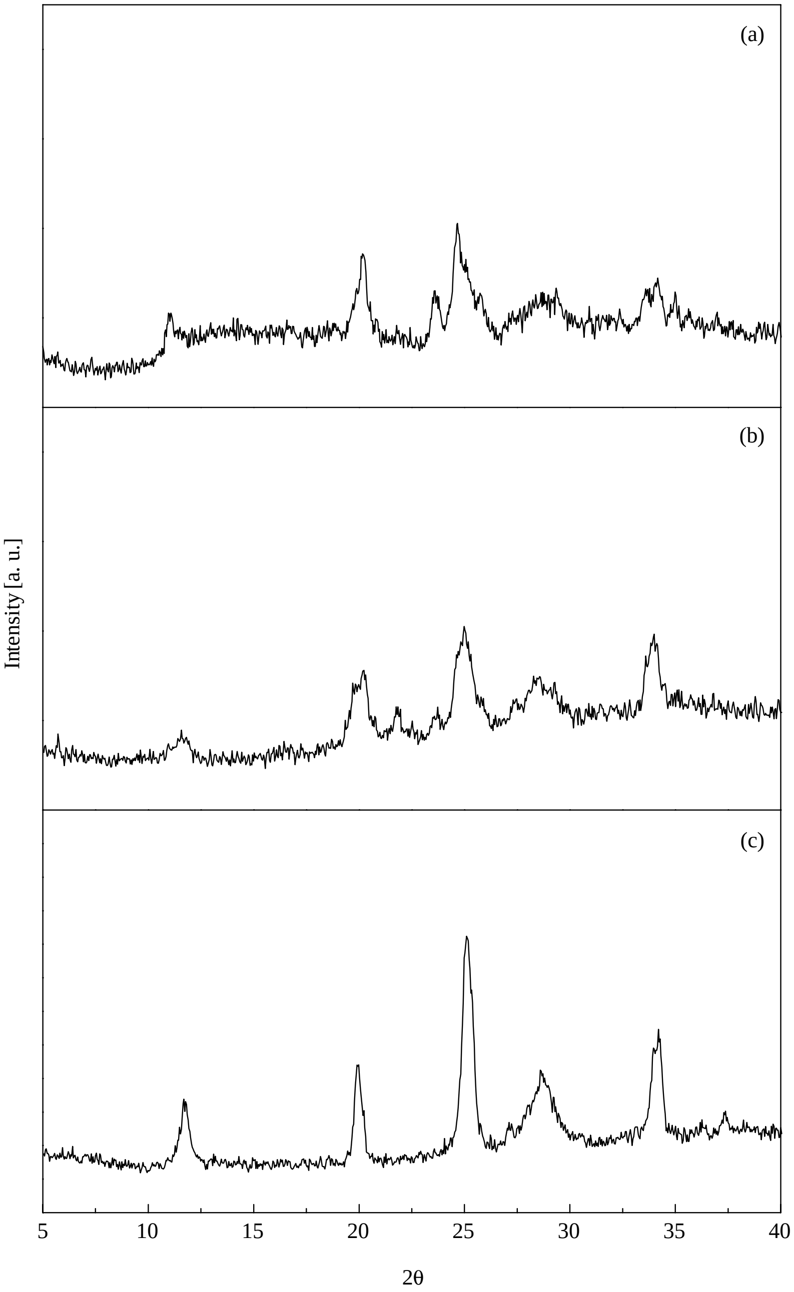

Fig. 8. XRDP of $SGZrPZnS_{450}$ at various sets of time flowing H_2S: (a) 15 h; (b) 25 h; (c) 50 h (see Fig. 5).

H_2S)/Zn^{2+} (from host matrix) does not occur in an acid environment.

3.5. Thermal behavior of SGZrPZnS

The TG curve of $SGZrPZnS_{450}$ (Fig. 5d) shows a weight loss due to dehydration and to S^{2-} combustion, respectively, at two distinct stages. The first stage occurs between 25 and 220 °C and the second between 220 and 700 °C. Water is lost at two stages, $0.56H_2O$ (25–80 °C) and $1.09H_2O$ (80–220 °C), in accordance with the two endothermic peaks on the DTA curve. S^{2-} elimination occurs at three different temperatures: 380–450–580 °C. The corresponding exothermic peaks are evident. This fact could be related to the different position of the ZnS particles in the SGZrP as was the case of CdS in the same host matrix [8b]. This is confirmed by the microanalysis measurements of the sulfur ions in the $SGZrPZnS_{450}$ materials heated at 380, 450, 580 °C which show a S^{2-} decrease as reported in Table 2. Note that at the above mentioned temperatures the decrease of S^{2-} eliminated is 0.13 (16.45%), 0.43 (54.43%) and 0.23 (29.12%) of the particles of the original number of ZnS. Few ZnS particles are on the surface of the SGZrP host matrix where lower temperature is sufficient to eliminate sulfur. The TG curve confirms these data. At 1000 °C an endothermic sharp peak, without weight loss, indicates syntherization. As far as $SGZrPZnS_{220}$ is concerned, its thermal behavior is similar to that reported in Fig. 5c: no S^{2-} combustion at 580 °C is evident. In the case of $SGZrPZn_{0.50}$ (Fig. 6), after the H_2S gas flow, the TG-DTA curves are similar to those of the original material $SGZrPZn_{0.50}$ (Fig. 1b) confirming the microanalysis data of Table 1.

3.6. XRD pattern of SGZrPZnS

As regards $SGZrPZnS_{220}$ and $SGZrPZnS_{450}$, the diffractograms are similar to those of SGZrP with another new peak at $2\theta = 28.50°$ due to the presence of ZnS particles [14], but different with respect to SGZrPZn material heated at 450 °C before the gas flow (Fig. 7). As far as $SGZrPZnS_{450}$ is concerned changes in the diffractograms take place gradually according to the length of time of the gas flow (Fig. 8). The material heated up to 350 °C, shows diffractograms similar to those of the SGZrP heated at the same temperatures (Fig. 5c). From 400 to 1100 °C, the XRD patterns are similar to those of SGZrPZn (Fig. 3) at the same temperature. The only difference between both (SGZrPZn and $SGZrPZnS_{450}$) is a shift of 1° or 0.5° in the peaks in the range $2\theta = 25–36°$ for the spectra recorded at 1100 °C.

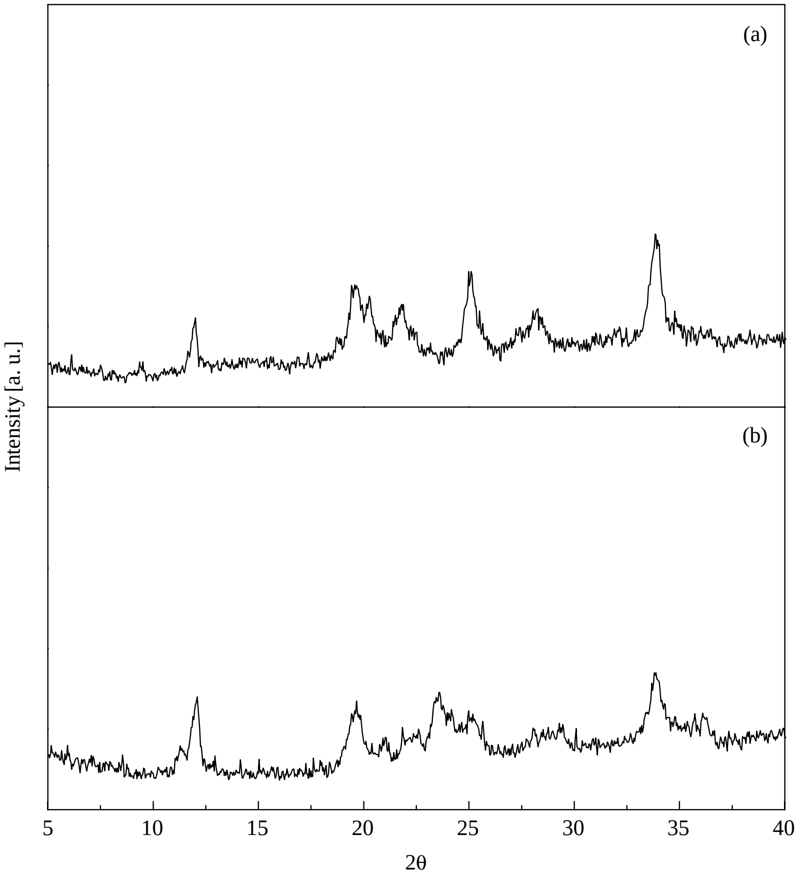

Fig. 9. XRDP of $SGZrPZn_{0.50}$ (a) and $SGZrPZn_{0.50}$ after gas flow (b) for comparison.

The diffractogram of $SGZrPZn_{0.50}$ after the gas flow (Fig. 9) is similar to that of Fig. 2b, but a little more amorphous.

4. Conclusions

Zinc ions can be exchanged in SGZrP (the α-zirconium phosphate synthesized using sol–gel method) by the batch or hydrothermal method. The fully and half exchanged forms that underwent the thermal treatment show a water loss due to the water co-ordination (25–220 °C). A transition phase (syntherization) exists at 1100 °C. After complete dehydration SGZrPZn and $SGZrPZn_{0.50}$ materials can be rehydrated up to 70 or 100%, respectively, if exposed to r.t. The XRD patterns show an increase in d (9.56 Å) with respect to its precursor SGZrP (7.56 Å) in the case of a fully exchanged form or a mixed phase (7.56 and 9.56 Å) in the case of a half exchanged one.

When anhydrous H_2S flows over the zinc materials, the zinc ions react to give ZnS particles. The number of the particles obtained depends on the hydration of the original SGZrPZn and on the length of time of the H_2S flow. As a result of microanalysis measurements, it has been ascertained that 0.79 mol ZnS/mol SGZrP are present in the fully exchanged form dehydrated at 450 °C, whereas the value for the partially dehydrated form, at 220 °C, is 0.57 mol ZnS/mol SGZrP. The half exchanged form does not "accept" the sulfur ions. The TG-DTA curves of the $SGZrPZnS_{450}$ material show water loss up to 220 °C. The heavy water loss at three distinct stages between 220 °C and 580 °C is related to the combustion and elimination of sulfur ions according to how the ZnS particles are bonded in the SGZrP host matrix. Maximum combustion occurs at 450 °C. As regards $SGZrPZnS_{220}$ material sulfur elimination occurs at two stages. The XRD pattern of the $SGZrPZnS_{450}$ shows a layered structure almost the same as its precursor SGZrP at r.t. and with evidence of the presence of ZnS particles at $2\theta = 28.50^\circ$. By recording its XRD patterns at various temperatures up to 400 °C the spectra are still similar to those of SGZrP, whereas up to 1100 °C the spectra are similar to those of SGZrPZn with insignificant differences.

Acknowledgements

Our sincere thanks to Dr. Patrizia Cafarelli (CNR, IMIP) for her help in preparing the samples and to Mrs. Gisella Menichelli (CNR, IMIP) for her great help in the bibliographical research.

References

[1] A. Clearfield (Ed.), Inorganic Ion-exchange Materials, vol. 20, CRC Press, Boca Raton, FL, 1982, Chapter 1 and references therein.
[2] (a) G. Alberti, U. Costantino, in: J.L. Atwood, J.E.D. Davies, D.D. Mac Nicol (Eds.), Inclusion Compounds, vol. 5, New York University Press, 1991, p. 136;
(b) K.J. Chao, et al., J. Mater. Chem. 3 (1993) 427;
(c) J. Votinsky, et al., J. Inclus. Phenom. 14 (1992) 19.
[3] C. Ferragina, et al., in: I.V. Mitchell (Ed.), Pillared Layered Structures, Elsevier, London, 1990, p. 127.
[4] (a) D.J. Jones, J. Roziere, Adv. Mater. Commun. 10 (1998) 812;
(b) Y. Ma, et al., Micropor. Mesopor. Mater. 37 (2000) 243.
[5] (a) A. Clearfield, J.A. Stynes, J. Inorg. Nucl. Chem. 26 (1964) 117;
(b) G. Alberti, E. Torracca, J. Inorg. Nucl. Chem. 30 (1968) 317;
(c) U. Costantino, A. La Ginestra, Thermochim. Acta 58 (1982) 179.
[6] (a) P. Giannoccaro, et al., in: H.U. Blaser, A. Baiker, R. Prins (Eds.), Heterogeneous Catalysis and Fine Chemicals, vol. IV, Elsevier, New York, 1997, p. 633;
(b) P. Giannoccaro, et al., J. Mol. Catal. 157 (1–2) (2000) 131.
[7] M. Turco, et al., J. Catal. 117 (1989) 355.
[8] (a) T. Cassagneau, et al., J. Mater. Chem. 4 (2) (1994) 189;
(b) C. Ferragina, et al., J. Therm. Anal. Calorim. 63 (2001) 709.
[9] (a) W.G. Becker, A.J. Bard, J. Phys. Chem. (1983) 4888;
(b) I. Dekany, et al., Langmuir 12 (1996) 3709;
(c) V. Stanic, et al., Mater. Lett. 31 (1997) 35.
[10] J. Livage, et al., J. Mater. Chem. 1 (4) (1991) 681.
[11] G. Alberti, et al., J. Inorg. Nucl. Chem. 28 (1966) 225.
[12] S. Allulli, et al., J. Chem. Soc., Dalton Trans. (1976) 2115.
[13] C. Bettinali, Atti Accad. Naz. Lincei, Sez. VIII (1962) 472.
[14] L.G. Berry (Ed.), Powder Diffraction File, JCPDS, File 36-1450, Philadelphia, 1974.